Computer-vision-based structural health monitoring of a truss structure subjected to unknown excitations: a robust framework

Mariusz OSTROWSKI[1], Bartlomiej BLACHOWSKI [1], Mateusz ŻARSKI [2], Piotr TAUZOWSKI[1], Łukasz JANKOWSKI[1]
[1]Institute of Fundamental Technological Research, Polish Academy of Sciences, Warsaw, Poland, mostr@ippt.pan.pl
[2]Institute of Theoretical and Applied Informatics, Polish Academy of Sciences, Gliwice, Poland

Abstract In this paper, a framework for computer-vision-based structural health monitoring (CVSHM) of truss structures under unknown load conditions is proposed. This framework is designed for highly contaminated measurement data, which are typical in CV measurements. The framework uses area-based template matching to extract nodal displacements from video, modal identification with SSI-DATA, automated rejection of out-of-plane vibration modes, automated rejection of gross errors, and model-updating-based damage assessment constrained to non-increasing stiffness with iterative rejection of structure members identified as non-damaged. The robustness to large measurement errors (up to 50 % RMS) is achieved. Excellent performance of the proposed framework is demonstrated on synthetic yet realistic videos and using available ground-truth data.

Keywords: model updating; inverse estimate; computer vision; robust damage assessment; structural health monitoring; non-negative least square method; physics-based graphical models

1. Introduction

Computer-vision-based structural health monitoring (CVSHM) enables non-contact, multi-point displacement measurement, reducing the cost and complexity of sensor installation. However, CV-based vibration measurements often suffer from strong noise, especially at high frequencies and low amplitudes [1, 2], motivating the development of noise-robust measurement and damage-assessment methods.

Template matching (TM) is widely used in CVSHM. Feature-based TM approaches match key points and are robust to lighting, scale, and rotation changes [3, 4]. Area-based approaches match pixel-intensity regions and offer higher precision under controlled conditions.

Modal data extracted from video can support damage detection. Due to highly contaminated measurements, this work focuses on model-based SHM. Classical model updating requires matching numerical and experimental modes [5, 6], which is difficult with a sparse sensor network or incomplete modal data. Minimizing the eigenvalue-equation imbalance avoids mode-matching issues but leads to ill-conditioned optimization, addressed through Bayesian maximum a posteriori estimation [7]. However, this method still can lead to numerical difficulties in some stiffness identification problems [8]. Regularization based on truncated singular value decomposition (TSVD) is also employed in classical approaches, with

https://doi.org/10.58286/33688

(a)

(b)

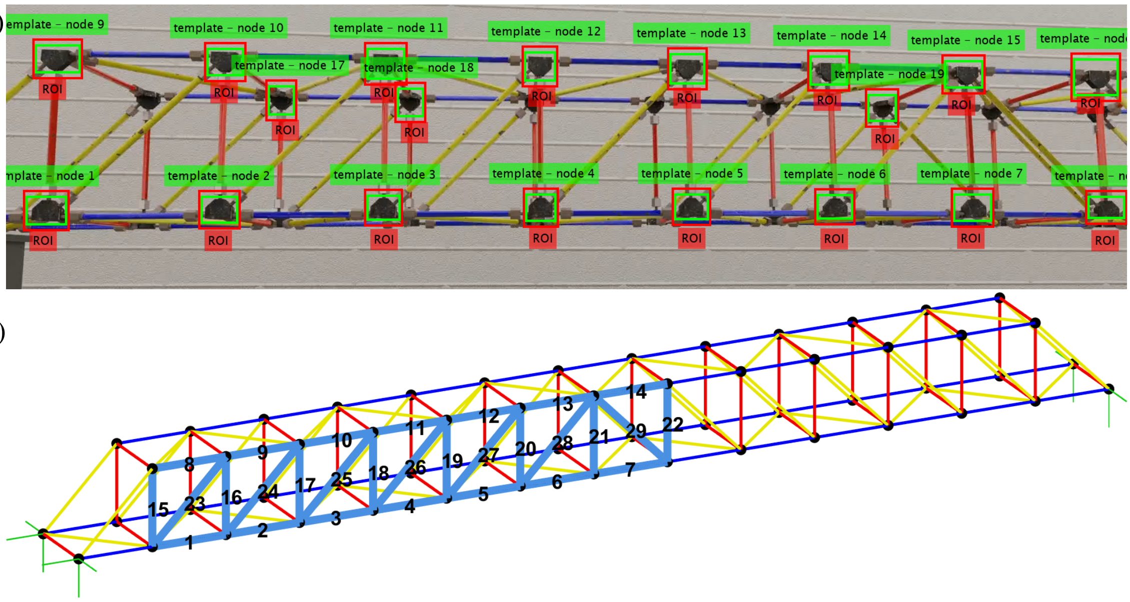

Fig. 1. *CVSHM of the considered truss structure: (a) selected templates and ROIs for estimation of nodal displacements in the synthetic video [12], and (b) finite-element model with indicated (blue color) and enumerated monitored elements*

additional rejection of gross errors [9]. Incorporating stiffness-reduction constraints significantly improves damage identification [10]. A recent method combines these ideas—iterative removal of undamaged members, optimality constraints, and weighting of modal parameters—achieving robust performance under heavy noise [11].

This paper evaluates the modified framework form [11] using synthetic yet realistic videos of a vibrating truss, based on physics-based graphical models (PBGM) [12]. Displacements are obtained via area-based template matching, followed by modal identification, automated gross-error rejection, and finite-element (FE) model updating using the weighted negative least-squares inverse estimate (WNLSIE). The framework enables the detection, localization, and quantification of damage even in the presence of 50% RMS noise.

2. Proposed Methodology for the Computer-vision-based Damage Assessment

2.1 Preparation of the data

Before estimation of nodal displacements, templates representing truss nodes and corresponding regions of interest (ROIs) are manually selected and saved. They are demonstrated, along with an example of a synthetic video frame, in Figure 1a.

As it is visible, the camera is not perpendicular to the structure plane. Hence, a homography transform is determined from points manually selected on the frame and known structure dimensions. Then, nodal positions can be expressed in the reference frame representing the perpendicular camera view. The pixel-to-meter scaling factor is also determined from the known structural dimensions.

2.2 Nodal Displacement Estimation

Structural displacements are estimated using area-based template matching. The template is matched with the actual position (x, y) of the truss node within the selected ROI by maximization of the zero-normalized cross-correlation function (ZNCC). The maximum of ZNCC is obtained via an exhaustive search. To achieve subpixel precision, ZNCC is additionally interpolated using a spline with a 16 times denser mesh of points.

2.3 Finite Element Model with Parametrized Stiffness

A parameterized FE model satisfies the equation of motion:

$$\begin{cases} \mathbf{M}\ddot{\mathbf{q}}(t) + \mathbf{C}\dot{\mathbf{q}}(t) + \mathbf{K}(\boldsymbol{\theta})\mathbf{q}(t) = \mathbf{f}(t) \\ \mathbf{y}(t) = \mathbf{D}\mathbf{q}(t) \end{cases}, \tag{1}$$

where: $\mathbf{M}$, $\mathbf{C}$, $\mathbf{K}(\boldsymbol{\theta})$ are mass, material damping, and parameterized stiffness matrices, respectively, $\mathbf{q}(t)$ is the displacement vector, $\mathbf{f}(t)$ is vector of external forces, which is unknown, $\mathbf{D}$ is Boolean matrix selecting the measured degrees of freedom (DOFs), and $\mathbf{y}(t)$ is output vector describing displacements corresponding with measured nodes shown in Figure 1a. The stiffness matrix $\mathbf{K}(\boldsymbol{\theta})$ depends on the stiffness parameters aggregated in vector $\boldsymbol{\theta} = \begin{bmatrix}\theta_1 & \cdots & \theta_{N_t}\end{bmatrix}^{\mathrm{T}}$ as follows:

$$\mathbf{K}(\boldsymbol{\theta}) = \mathbf{K}_0 + \sum_{t=1}^{N_t} \theta_t \mathbf{K}_t, \tag{2}$$

where $\mathbf{K}_0$ represents the stiffness of the part of the structure, which is not monitored, whereas $\mathbf{K}_t$ describes the stiffness of a particular monitored element t. Initially, all $\theta_t = 1$. The damaged element has a stiffness parameter identified as smaller than 1. Then, the damage index is defined as:

$$\mathrm{DI}_t = 1 - \theta_t. \tag{3}$$

The FE model of the considered truss structure is shown in Figure 1b along with boundary conditions and monitored structural members (corresponding with matrices $\mathbf{K}_t$).

Beam-type FEs based on Euler-Bernoulli beam theory with cubic shape functions are used. The structure has a length of 5.5118 m, a height of 0.4 m, and a width of 0.3937 m. Structural members are pipes of outer and inner diameters 0.01554 m and 0.01087 m, respectively. Young modulus is 18.5 GPa, and material density is 8000 kg/m^3.

2.4 Identification of Structural Vibration Modes

Structure is excited by unknown forces. Only the displacements extracted from the video frames are available. Thus, the data-driven stochastic subspace identification method (SSI-DATA) is employed to identify structural vibration modes [13]. Stabilization diagrams are used to remove spurious modes. The procedure employing stabilization diagrams for data obtained with CV is described in detail in [11, 14].

As out-of-plane vibration modes are not well observed by the camera, they are rejected. To assess if the identified vibration mode is out-of-plane, the following criterion employing the FE model of the structure is used:

$$\frac{\left\|\mathbf{D}_z \boldsymbol{\phi}^{(n)}(\boldsymbol{\theta})\right\|_1}{\left\|\mathbf{D}_y \boldsymbol{\phi}^{(n)}(\boldsymbol{\theta})\right\|_1} \leq \kappa_{YZ}, \tag{4}$$

where: $\|\cdot\|_1$ denotes the the $\ell 1$-norm, $\mathbf{D}_z$ and $\mathbf{D}_z$ are output Boolean matrices selecting the horizontal (perpendicular to the truss plane) and vertical DOFs from the FE model, respectively, and $\boldsymbol{\phi}^{(n)}(\boldsymbol{\theta})$ is numerical mode shape matched with the experimentally identified one $\widehat{\boldsymbol{\phi}}^{(m)}$ according to the following criterion:

$$n = \arg\max_{p} \left[\mathrm{MAC}\left(\widehat{\boldsymbol{\phi}}^{(m)}, \mathbf{D}\boldsymbol{\phi}^{(p)}(\boldsymbol{\theta})\right) - 2\frac{\left(\widehat{\lambda}^{(m)} - \lambda^{(p)}(\boldsymbol{\theta})\right)^2}{\widehat{\lambda}^{(m)\,2}} \right], \tag{5}$$

where: $\mathrm{MAC}(\cdot,\cdot)$ is modal assurance criterion, $\widehat{\lambda}^{(m)} = \left(2\pi \widehat{f}^{(m)}\right)^2$ is mth eigenvalue identified experimentally, $\widehat{f}^{(m)}$ is corresponding natural frequency, and $\lambda^{(p)}(\boldsymbol{\theta})$ is pth numerical eigenvalue calculated analogously.

2.5 Proposed Robust Damage Assessment Method

The proposed robust damage assessment method is based on a weighted negative least-squares inverse estimate, in which the optimization problem linearized with respect to $\Delta\boldsymbol{\theta}$ is solved in each algorithm iteration:

$$\begin{array}{ll} \text{find} & \Delta\boldsymbol{\theta} \\ \text{to minimize} & \|\mathbf{S}(\boldsymbol{\theta})\Delta\boldsymbol{\theta} - \mathbf{e}(\boldsymbol{\theta})\|^2_{\mathbf{W}} \\ \text{subject to} & \Delta\theta_t \le 0, \quad t = 1, 2, \ldots N_t, \end{array} \tag{6}$$

where: $\Delta\boldsymbol{\theta}$ is the change of parameter vector, $\|\cdot\|_{\mathbf{W}}$ is $\ell 2$-norm with respect to a weighting matrix $\mathbf{W}$, $\mathbf{S}(\boldsymbol{\theta})$ is modal sensitivity matrix collecting derivatives of the system eigenvalues $\frac{\partial\lambda^{(n)}}{\partial\theta_t}$ and mode shapes at monitored locations (Fig. 1a) $c_m \mathbf{D}_z \frac{\partial\boldsymbol{\phi}^{(n)}}{\partial\theta_t}$, $t = 1 \ldots N_t$, which are calculated according to [15], and [16], respectively,

$$c_m = \frac{\widehat{\boldsymbol{\phi}}^{(m)\mathrm{T}} \mathbf{D}_z \boldsymbol{\phi}^{(n)}}{\left\|\mathbf{D}_z \boldsymbol{\phi}^{(n)}\right\|^2} \tag{7}$$

is the modal scale factor,

$$\mathbf{e}(\boldsymbol{\theta}) = \begin{bmatrix} \widehat{\boldsymbol{\lambda}} \\ \widehat{\boldsymbol{\phi}} \end{bmatrix} - \begin{bmatrix} \boldsymbol{\lambda}(\boldsymbol{\theta}) \\ \boldsymbol{\phi}(\boldsymbol{\theta}) \end{bmatrix} \tag{8}$$

is error between modal parameters obtained experimentally and numerical ones, where: $\widehat{\boldsymbol{\lambda}} = \left[\widehat{\lambda}^{(1)} \ \cdots \ \widehat{\lambda}^{(N)}\right]^{\mathrm{T}}$, $\boldsymbol{\lambda}(\boldsymbol{\theta}) = \left[\lambda^{(n_1)}(\boldsymbol{\theta}) \ \cdots \ \lambda^{(n_N)}(\boldsymbol{\theta})\right]^{\mathrm{T}}$, $\widehat{\boldsymbol{\phi}} = \left[\widehat{\boldsymbol{\phi}}^{(1)\mathrm{T}} \ \cdots \ \widehat{\boldsymbol{\phi}}^{(N)\mathrm{T}}\right]^{\mathrm{T}}$, and $\boldsymbol{\phi}(\boldsymbol{\theta}) = \left[[c_1 \mathbf{D}_z \boldsymbol{\phi}^{(n_1)}(\boldsymbol{\theta})]^{\mathrm{T}} \ \cdots \ [c_N \mathbf{D}_z \boldsymbol{\phi}^{(n_N)}(\boldsymbol{\theta})]^{\mathrm{T}}\right]^{\mathrm{T}}$. In the optimization problem above, only transversal DOFs are considered (corresponding to the output matrix $\mathbf{D}_z$) are taken into account, as they have greater motion amplitudes in relation to the measurement noise in the considered videos. Aiming at proper weighting of the error norm in the objective function, the weighting matrix reciprocal to the covariance matrix can be employed. As the covariance matrix is not known in this study, $\mathbf{W}$ is selected as reciprocal to the typical relative errors of modal parameters:

$$\mathbf{W} = \mathrm{diag}\left(\left[\frac{1}{\widehat{\lambda}^{(1)2}} \ \cdots \ \frac{1}{\widehat{\lambda}^{(N_m)2}} \ \frac{\nu_\phi^2 N_z}{\left\|\widehat{\boldsymbol{\phi}}^{(1)}\right\|^2}\mathbf{1}_\phi^{\mathrm{T}} \ \cdots \ \frac{\nu_\phi^2 N_z}{\left\|\widehat{\boldsymbol{\phi}}^{(N_m)}\right\|^2}\mathbf{1}_\phi^{\mathrm{T}}\right]^{\mathrm{T}}\right), \tag{9}$$

where: N_z is the number of measured transversal DOFs, $\mathbf{1}_\phi$ is vector of ones of appropriate dimension, and ν_ϕ is selected coefficient, usually $\nu_\phi \ll 1$. Such a weighting matrix not only

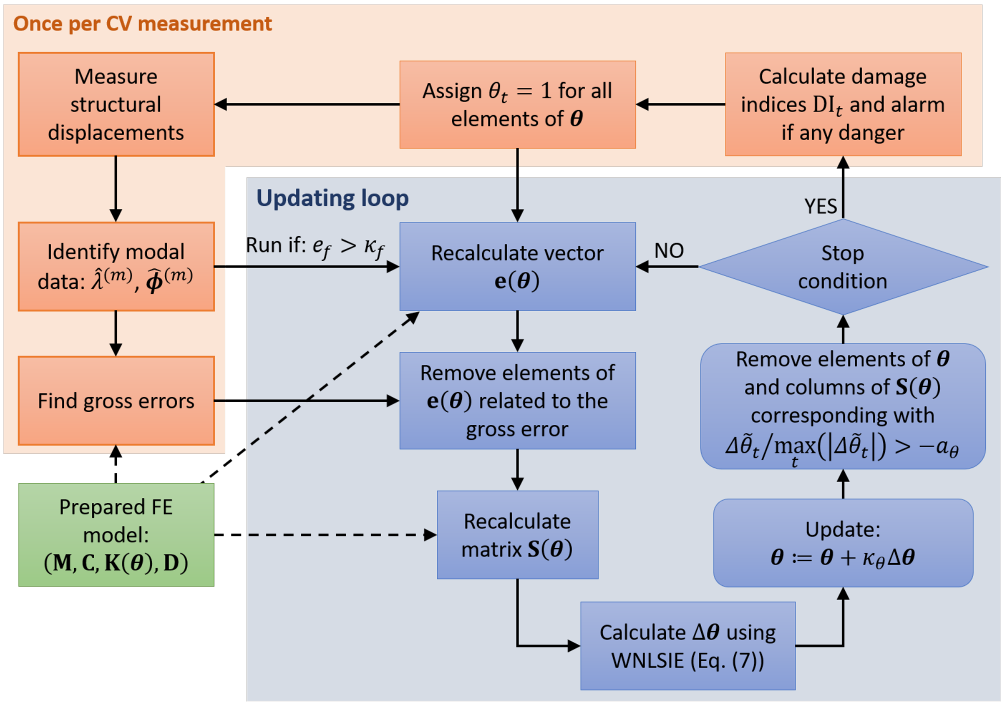

Fig. 2. *Flow chart of the proposed SHM algorithm*

quantifies errors but also improves the problem's numerical conditioning. After some equation modifications, nonnegative-linear-least-squares solvers can be used to solve the problem in Eq. (6).

Aiming at the robust estimate of structural stiffness in the presence of large measurement errors, WNLSIE is implemented in the algorithm shown in Figure 2. The updating loop is run only if the root-mean-square (RMS) value of the relative frequency error is greater than the preselected threshold κ_f:

$$e_f = \mathrm{RMS}\left(\frac{\widehat{f}^{(m)} - f^{(n)}(\boldsymbol{\theta})}{\widehat{f}^{(m)}}\right) > \kappa_f. \tag{10}$$

Identified mode shapes highly contaminated by measurement noise in CV measurement are detected and removed from vector $\mathbf{e}(\boldsymbol{\theta})$ and matrix $\mathbf{S}(\boldsymbol{\theta})$. The criterion is that the MAC between the identified mode shape and the matched mode shape of the undamaged FE model is less than 0.8, with only vertical displacements considered. It is assumed that elements of $\boldsymbol{\theta}$ whose changes are smaller than α_θ in relation to the biggest change correspond to undamaged elements and are removed from the model-updating procedure. It iteratively reduces the search space and significantly improves computational accuracy. The stop condition is $\max_t |\Delta\theta_t| < \alpha_{\mathrm{tol}\,\theta}$

3. Results

Synthetic Full HD-resolution videos, 4 min long and sampled at 120 frames per second, are considered. Figure 3 compares vertical displacements extracted from the video using the adopted template-matching method with the ground-truth data for measurement nodes no. 8 and 9 (see Fig. 1a) for a healthy structure. As the node no. 8 has a relatively big amplitude of motion, the measurement error is relatively small. On the contrary, node no. 9, which is located close to the support and at the top of the structure, has a small motion amplitude.

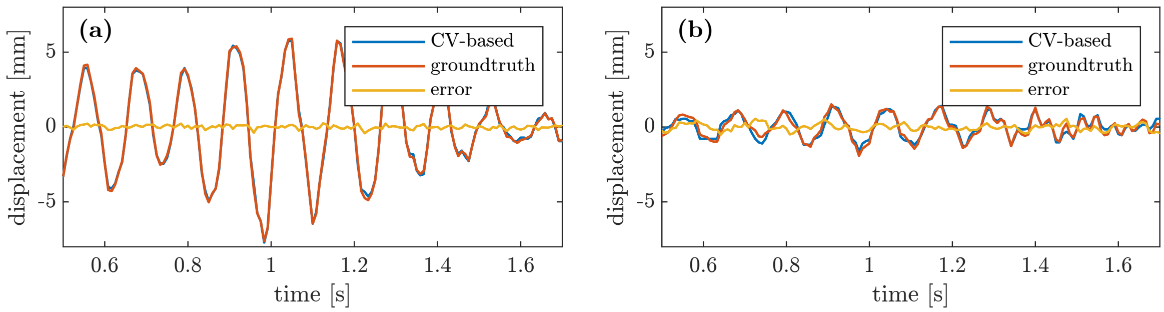

Fig. 3. *Comparison of the extracted vertical displacement with ground-truth data for (a) node no. 8 (in the structure middle) and (b) node no. 9 (close to the support)*

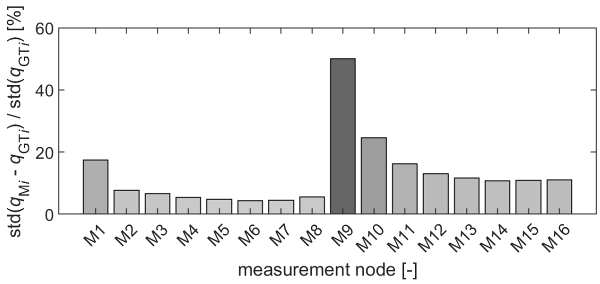

Fig. 4. *Standard deviation of measurement error of vertical displacement in relation to the standard deviation of ground truth for measurement nodes 1-16*

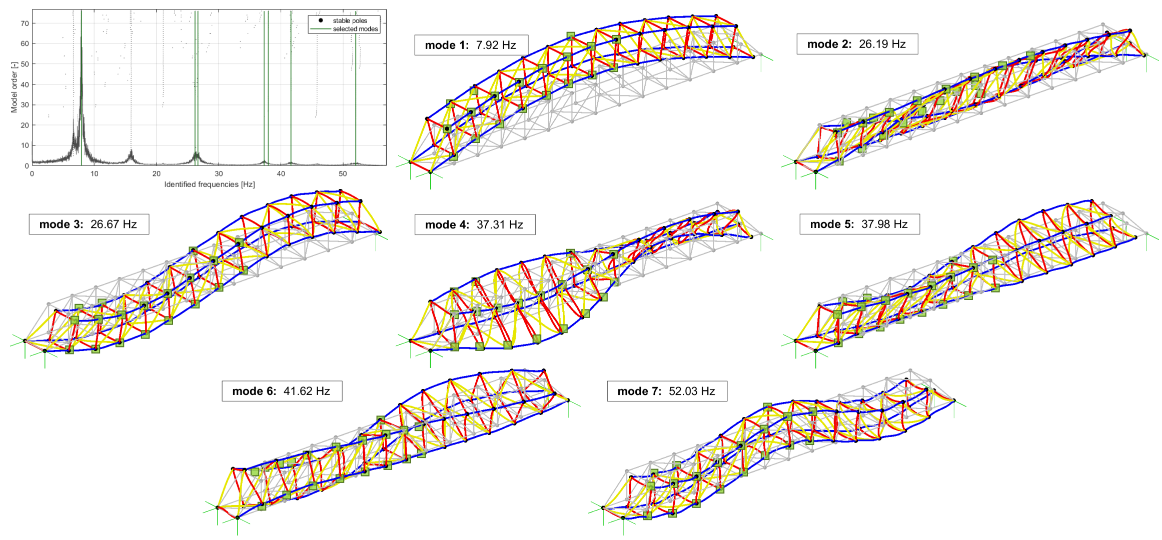

Fig. 5. *SSI-DATA-based identification of in-plane vibration modes of the undamaged structure: stabilization diagram and vibration modes 1-7 (green squares) with matched numerical ones (FE model)*

This motion contains components related to out-of-plane modes, which are visible due to location of the node near to the corner of the video-frame. It results in greater measurement error values: both absolute and in relation to the signal level. This dependence is visible for all measurement nodes. Figure 4 shows that the standard deviation of measurement error is 15–50 % of the ground-truth standard deviation for the nodes located on the top and close to the structural support.

An example of the stabilization diagram and the identified mode shapes selected according to the criteria described in Subsection 2.4 for the undamaged structure is shown in Figure 5. Parameter $\kappa_{XY} = 0.8$ was selected.

10 basic damage scenarios are available in the set of synthetic videos. Results of damage assessments of monitored elements (see: Fig. 1b) compared with the ground-truth data for selected "Damage 4" and "Damage 6" scenarios are shown in Figure 6. The algorithm

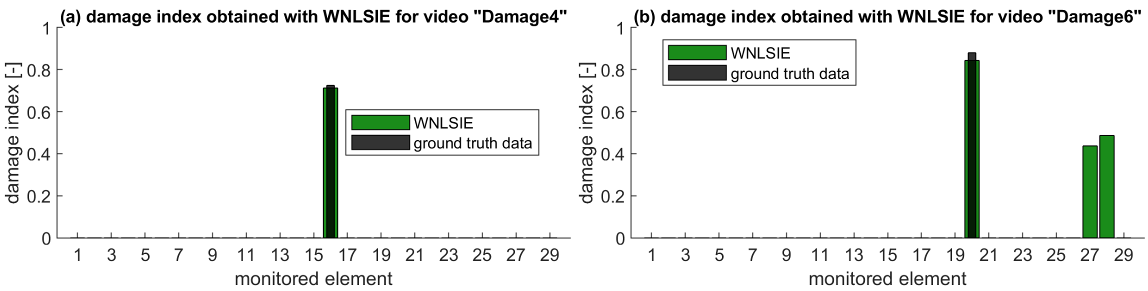

Fig. 6. *Comparison of estimated damage indices and the ground truth data for selected damage cases*

was run with the following parameters, selected via trial and error: $\nu_\phi = 0.025$, $\kappa_f = 0.5$ %, $\kappa_\theta = 0.25$, $\alpha_\theta = 0.4$, and $\alpha_{\mathrm{tol}\,\theta} = 10^{-3}$. In both cases, the damage is correctly indicated and its level assessed with satisfactory accuracy. Given the large CV measurement errors and the relatively large number of monitored structural members (29 unknown stiffness parameters), the sparsity of the damage index is also satisfactory, with false-positive damage indices occurring rarely. Among the 10 basic damage scenarios, only in the video “Damage 8” is the damaged element incorrectly localized.

4. Conclusions

The proposed framework for CVSHM is robust to large measurement noise. Attention is paid to removing out-of-plane vibration modes, removing gross errors from identified modal parameters, imposing constraints on the optimization problem, and iteratively reducing the parameter search space. All of these elements improve the robustness and accuracy of the damage assessment. The tests on synthetic videos demonstrate that the proposed framework can monitor a relatively large number of structural members in the presence of large measurement error, even up to 50 % of the signal RMS.

In one damage scenario, the damage is mislocated. Hence, despite its high robustness, the proposed framework still requires improvement. Additionally, many algorithm parameters are selected with trial and error. Thus, their elimination from the framework, or the methods of their selection, should be proposed. These are problems to be undertaken in future research.

References

[1] Yuansheng Cheng, Zhe Tian, Donghong Ning, Ke Feng, Zhixiong Li, Sumika Chauhan, and Govind Vashishtha. Computer vision-based non-contact structural vibration measurement: Methods, challenges and opportunities. *Measurement*, 243:116426, 2025.

[2] F. Trainotti, T. Slimak, and D. Rixen. Towards full-field frequency based substructuring: an application case. In *International Conference on Noise and Vibration Engineering and International Conference on Uncertainty in Structural Dynamics (ISMA 2022 – USD 2022).*, 2022.

[3] Dongming Feng and Maria Feng. *Computer Vision for Structural Dynamics and Health Monitoring*. John Wiley & Sons Ltd and ASME Press, 2021.

[4] Bartlomiej Blachowski, Mariusz Ostrowski, Mateusz Żarski, Bartosz Wójcik, Piotr Tauzowski, and Łukasz Jankowski. An efficient computer vision-based method for estimation of dynamic displacements in spatial truss structures. In Piervincenzo Rizzo and Alberto Milazzo, editors, *European Workshop on Structural Health Monitoring (EWSHM 2023)*, pages 474–484. Springer International Publishing, 2023.

[5] Michael Friswell and J. E. Mottershead. *Finite Element Model Updating in Structural Dynamics*. Springer, Dordrecht, 1995.

[6] J K Sinha and M I Friswell. Model updating: A tool for reliable modelling, design modification and diagnosis. *Shock and Vibration Digest*, 34(1):27–35, 1 2002.

[7] Ka-Veng Yuen, James L Beck, and Lambros S Katafygiotis. Efficient model updating and health monitoring methodology using incomplete modal data without mode matching. *Structural Control and Health Monitoring*, 13:91–107, 2006.

[8] Mariusz Ostrowski, Grzegorz Mikułowski, Bartłomiej Błachowski, and Łukasz Jankowski. Experimental assessment of bayesian and mode matching approaches for parametric identification of bolted connections. *Mechanical Systems and Signal Processing*, 201:110652, 2023.

[9] X Peng, F J Qin, Q W Yang, and H Chen. A robust estimate method for damage detection of concrete structures using contaminated data. *Advances in Civil Engineering*, 2021:6669958, 2021.

[10] Bartlomiej Blachowski. Modal sensitivity based sensor placement for damage identification under sparsity constraint. *Periodica Polytechnica Civil Engineering*, 63:432–445, 2019.

[11] Mariusz Ostrowski, Bartlomiej Blachowski, Bartosz Wó'jcik, Mateusz Żarski, Piotr Tauzowski, and Łukasz Jankowski. A framework for computer vision-based health monitoring of a truss structure subjected to unknown excitations. *Earthquake Engineering and Engineering Vibration*, 22:1–17, 2023.

[12] Yasutaka Narazaki, Fernando Gomez, Vedhus Hoskere, Matthew D Smith, and Billie F Spencer. Efficient development of vision-based dense three-dimensional displacement measurement algorithms using physics-based graphics models. *Structural Health Monitoring*, 20:1841–1863, 2021.

[13] Bart Peeters. *System identification and damage detection in civil engineering*. PhD thesis, 2000.

[14] Mariusz Ostrowski, Bartlomiej Blachowski, Grzegorz Mikułowski, and Łukasz Jankowski. Influence of noise in computer-vision-based measurements on parameter identification in structural dynamics. *Sensors*, 23, 2023.

[15] R L Fox and M P Kapoor. Rates of change of eigenvalues and eigenvectors. *AIAA Journal*, 6:2426–2429, 1968.

[16] Richard B Nelson. Simplified calculation of eigenvector derivatives. *AIAA Journal*, 14:1201–1205, 1976.